Efficient and robust calculation of femtoscopic correlation functions in spherical harmonics directly from the raw pairs measured in heavy-ion collisions

A. Kisiel
Department of Physics, The Ohio State University, Columbus, Ohio 43210, USA

D. A. Brown
Lawrence Livermore National Laboratory, Livermore, California 94551, USA

(Received 22 January 2009; published 28 December 2009)

We present the formalism for calculating the femtoscopic correlation function directly in spherical harmonics. The numerator and denominator are stored as a set of one-dimensional histograms representing the spherical harmonic decompositions of each. We present the formalism to calculate the correlation function from them directly, without going to any three-dimensional histogram. We discuss the practical implementation of the method and we provide an example of its use. We also discuss the stability of the method in the presence of angular holes in the underlying data (e.g., from experimental acceptance).

DOI: 10.1103/PhysRevC.80.064911 PACS number(s): 25.75.Gz, 24.10.−i

Spherical harmonics are one of the most commonly used mathematical tools for the analysis of experimental data. For example, geopotential models of Earth's gravitational field are matched to experimental data up to harmonic order $\ell_{\max} = 70$ [1]. Measurements of the cosmic microwave background by the Cosmic Background Explorer (COBE) [2] and successor experiments extend further to an impressive $\ell_{\max} \approx 1500$ [3]. In the femtoscopic measurements of particle-emitting sources in heavy-ion collisions, one also finds it useful to expand the measured correlations and extracted sources in spherical harmonics [4,5].

In nearly all applications of spherical harmonics to data analysis and reduction, one is faced with the problem of "holes in the data" (i.e., sampling bias [6]). In the COBE analysis mentioned above, this bias occurs because the Milky Way masks a sizable solid angle of the sky. When constructing potential maps of Earth, the problem is even more severe as one uses strips of data obtained from various satellite and balloon-borne experiments to derive the map [7]. In heavy-ion collisions, the sampling bias most often arises because the detector acceptance does not span all of phase space.

Unlike other applications, the femtoscopic correlation functions are actually ratios of two single-particle distributions: the true pair distribution (the numerator) and the mixed pair distribution (the denominator). Thus, expanding the correlation function in spherical harmonics is more involved than expanding the underlying single-particle distributions. It is often impractical to simply bin the two single distributions in 3D histograms and make a ratio because one does not have a meaningful number of pairs in each bin, attributable either to the statistics of particle production or to detector acceptances. Furthermore, because the end result is a spherical harmonic decomposition of the correlation, one must have absurdly high harmonics in one's decomposition to resolve high-momentum bins that have small angular extent and marginal statistics.

Rather than pursue this, we adopt an alternate approach: We construct the raw-pair distributions directly in spherical harmonics, then we extract the correlation function, also in spherical harmonics, by viewing the ratio as an inverse problem. A feature of this approach is that one preserves the full cross-ℓ, m data covariance that is currently ignored when imaging 3D correlations [4].

We now outline this article. In the first section, we detail how we expand the numerator and denominator distributions in spherical harmonics and how we pack them into the vectors and matrices for further manipulation. In the second section, we describe how to compute the correlation in spherical harmonics using these harmonic expansions. In the last section, we demonstrate the technique in realistic examples. Further, we show how this technique is insensitive to the sampling bias imposed by sizable holes in pair acceptance.

I. CONSTRUCTING THE NUMERATOR AND DENOMINATOR

The femtoscopic correlation function, $C(\mathbf{q})$, is defined as a ratio of the probability to observe a correlated pair of particles at a given relative momentum in the same event (numerator), $T(\mathbf{q})$, to the probability to observe such a pair in an uncorrelated state (denominator), $M(\mathbf{q})$:

$$T(\mathbf{q}) = C(\mathbf{q})M(\mathbf{q}). \tag{1}$$

The uncorrelated distribution is usually obtained by mixing particles from different events. Here the relative momentum is given in the pair center of mass frame as $\mathbf{q} = \frac{1}{2}(\mathbf{p_1} - \mathbf{p_2}) = \mathbf{k}^*$ for particles 1 and 2. Here $\mathbf{k}^*$ is the notation commonly used for femtoscopic correlations for pairs of two different types of particles and will be used interchangeably with $\mathbf{q}$ (traditionally used in femtoscopic correlations of pairs of identical particles) later in the article. We expand the numerator, denominator, and correlation function in spherical harmonics; for example,

$$T(\mathbf{q}) = \sqrt{4\pi} \sum_{\ell m} T_{\ell m}(q) Y_{\ell m}(\Omega_{\hat{\mathbf{q}}}). \tag{2}$$

TABLE I. Conditions on the distribution imply relations between the different terms in the $Y_{\ell m}$ expansion. Condition 1 is always valid for the true and mixed pair distributions and the correlation function. Condition 5 is always valid for like-pair correlation and the corresponding pairs distributions. By exploiting symmetries in conditions 2–5, we can reduce the number of components in our data vectors.

	Condition	Relation
1	Distribution is real	$T_{\ell m} = T^*_{\ell -m}$
2	$x \to -x$ symmetry	$T_{\ell m}(x, y, z) = (-1)^m T^*_{\ell m}(-x, y, z)$
3	$y \to -y$ symmetry	$T_{\ell m}(x, y, z) = T^*_{\ell m}(x, -y, z)$
4	$z \to -z$ symmetry	$T_{\ell m}(x, y, z) = (-1)^{\ell+m} T_{\ell m}(x, y, -z)$
5	$\mathbf{r} \to -\mathbf{r}$ symmetry	$T_{\ell m}(x, y, z) = (-1)^{\ell} T_{\ell m}(-x, -y, -z)$

We can compute the pairs distributions directly in spherical harmonics by observing that

$$T_{\ell m}(q) = \frac{1}{\sqrt{4\pi}} \int_{4\pi} d\Omega_{\hat{\mathbf{q}}} T(\mathbf{q}) Y^*_{\ell m}(\Omega_{\hat{\mathbf{q}}}) \tag{3}$$

can be built up by summing over the pairs, which is essentially a Monte-Carlo integration process:

$$T_{\ell m}(q_n) \approx \frac{\sqrt{4\pi}}{N} \sum_{i=1}^{N} \begin{cases} Y^*_{\ell m}(\Omega_{\hat{\mathbf{q}}_i}) & \text{if } q_i \text{ in bin } n, \\ 0 & \text{otherwise.} \end{cases} \tag{4}$$

Here, N is the number of pairs in the spectrum. In our approach, a pair is added to $T_{\ell m}(q_n)$ $[M_{\ell m}(q_n)]$ in the following way. First we calculate the relative momentum $\mathbf{q}$ and decompose it into $|\mathbf{q}|$ (which determines the 1D q-bin number), $\theta_{\hat{\mathbf{q}}_i}$, and $\phi_{\hat{\mathbf{q}}_i}$. Having the angles, we can calculate the spherical harmonics functions, usually up to some limiting value of ℓ. Then the pair is added to all histograms of the corresponding function, with weights equal to the respective $Y_{\ell m}$'s. We could eliminate many of the components of $T_{\ell m}(q_n)$ and $M_{\ell m}(q_n)$ by taking advantage of the symmetries in Table I, but we have chosen to keep all components so that we can perform cross-checks of our work. This does introduce complications when performing some matrix manipulations, as we discuss in the following section.

The covariance can be built in a similiar way by noting (if q_i in radial bin n only)

$$\Delta^2 T_{\ell m \ell' m'}(q_n) \approx \frac{4\pi}{N(N-1)} \sum_{i=1}^{N} \left[Y^*_{\ell m}(\Omega_{\hat{\mathbf{q}}_i}) - \frac{T_{\ell m}(q_n)}{\sqrt{4\pi}} \right] \times \left[Y^*_{\ell' m'}(\Omega_{\hat{\mathbf{q}}_i}) - \frac{T_{\ell' m'}(q_n)}{\sqrt{4\pi}} \right]^*. \tag{5}$$

Taking the diagonal elements (i.e., $\ell m = \ell' m'$), we find (uncorrelated) uncertainties of

$$\Delta T_{\ell m}(q_n) \approx \sqrt{\Delta^2 T_{\ell m \ell m}(q_n)}. \tag{6}$$

In contrast with our approach, in the traditional representation both the numerator and the denominator were stored as 3D histograms, using either the Bertsch-Pratt coordinates [8] in Cartesian form q_{out}, q_{side}, and q_{long} or in spherical form $|\mathbf{q}|$, $\cos(\theta_{\hat{\mathbf{q}}})$, $\phi_{\hat{\mathbf{q}}}$. In the traditional representation the numerator (denominator) is a 3D histogram, and each signal (background) pair is added to exactly one bin of this histogram with weight 1.0. This representation has several disadvantages: one needs significant statistics to have a meaningful number of pairs in each bin, single-particle momentum acceptance can result in "holes" or empty bins in two-particle, or relative momentum space, and the binning corrections need to be applied. Also going to higher moments in the decomposition requires larger number of bins on the $\phi_{\hat{\mathbf{q}}}$ and $\theta_{\hat{\mathbf{q}}}$ direction.

In practice, we store both the real and the imaginary parts of the numerator and the denominator as an array of 1D histograms in $q = |\mathbf{q}|$, as seen in Eq. (7), which is represented as the vector $\mathbf{T}_q$:

$$\mathbf{T}_q = \begin{pmatrix} T_{00}(q) \\ T_{10}(q) \\ \Re T_{11}(q) \\ \Im T_{11}(q) \\ T_{20}(q) \\ \Re T_{21}(q) \\ \Im T_{21}(q) \\ \Re T_{22}(q) \\ \Im T_{22}(q) \\ T_{30}(q) \\ \vdots \end{pmatrix}. \tag{7}$$

There is also a corresponding covariance matrix $\mathbf{\Delta}^2 \mathbf{T}_q$, which is a 2D matrix for each q bin and is packed in an analogous fashion.

II. CALCULATING THE CORRELATION FUNCTION

Because we have expanded the pair distributions and the correlation in spherical harmonics, we have

$$\begin{aligned} T_{\ell m}(q) &= \sum_{\ell' m' \ell'' m''} M_{\ell' m'}(q) C_{\ell'' m''}(q) \\ &\quad \times \int_{4\pi} d\Omega_{\hat{\mathbf{q}}} Y^*_{\ell m}(\Omega_{\hat{\mathbf{q}}}) Y_{\ell' m'}(\Omega_{\hat{\mathbf{q}}}) Y_{\ell'' m''}(\Omega_{\hat{\mathbf{q}}}) \\ &\equiv \sum_{\ell'' m''} \tilde{M}_{\ell m \ell'' m''}(q) C_{\ell'' m''}(q). \end{aligned} \tag{8}$$

With the packing in Eq. (7), Eq. (8) can be written very compactly: $\mathbf{T}_q = \tilde{\mathbf{M}}_q \cdot \mathbf{C}_q$. Equation (8) gives us a way to compute $C_{\ell m}(q)$ directly from the pair distributions expanded in spherical harmonics.

Here the $\tilde{\mathbf{M}}_q$ matrix is written in terms of Wigner 3-j symbols as

$$\begin{aligned} \tilde{M}_{\ell m \ell'' m''} &= \sum_{\ell' m'} M_{\ell' m'}(q) (-1)^m \sqrt{(2\ell+1)(2\ell'+1)(2\ell''+1)} \\ &\quad \times \begin{pmatrix} \ell & \ell' & \ell'' \\ 0 & 0 & 0 \end{pmatrix} \begin{pmatrix} \ell & \ell' & \ell'' \\ -m & m' & m'' \end{pmatrix}. \end{aligned} \tag{9}$$

To calculate the correlation function, we view the problem as an inverse problem. To solve it, one needs to minimize

the χ^2:

$$(\mathbf{T}_q - \tilde{\mathbf{M}}_q \cdot \mathbf{C}_q)^T \cdot (\boldsymbol{\Delta}^2\mathbf{T}_q)^{-1} \cdot (\mathbf{T}_q - \tilde{\mathbf{M}}_q \cdot \mathbf{C}_q). \quad (10)$$

The formula uses the full covariance matrix in the true distribution, but not in the mixed pair distribution. Because the mixed pair distribution is constructed by pairs from different events, it is not limited by statistics and can be computed to arbitrarily high precision, making the uncertainties negligible for our purposes. The problem of minimizing the χ^2 is identical to the one posed by the imaging procedure in Ref. [4] and the solution is well known:

$$\mathbf{C}_q = \boldsymbol{\Delta}^2\mathbf{C}_q \cdot \tilde{\mathbf{M}}_q^T \cdot (\boldsymbol{\Delta}^2\mathbf{T}_q)^{-1} \cdot \mathbf{T}_q, \quad (11)$$

where the covariance is also calculated:

$$\boldsymbol{\Delta}^2\mathbf{C}_q = \left(\tilde{\mathbf{M}}_q^T \cdot (\boldsymbol{\Delta}^2\mathbf{T}_q)^{-1} \cdot \tilde{\mathbf{M}}_q\right)^{-1}. \quad (12)$$

The uncorrelated uncertainties of the correlation are just the square root of the trace of the covariance $\boldsymbol{\Delta}^2\mathbf{C}_q$: $\boldsymbol{\Delta}\mathbf{C}_q = \sqrt{\mathrm{Tr}\boldsymbol{\Delta}^2\mathbf{C}_q}$. Written out, we are simply taking the diagonal elements (i.e., $\ell m = \ell' m'$) and finding (uncorrelated) uncertainties of

$$\Delta C_{\ell m}(q_n) \approx \sqrt{\Delta^2 C_{\ell m \ell m}(q_n)}. \quad (13)$$

With the error propagation done in this way, one gets the cross-ℓm correlations in the covariance matrix by virtue of the cross-ℓm correlations built into the $\tilde{\mathbf{M}}_q$ and $\boldsymbol{\Delta}^2\mathbf{T}_q$ matrices.

We compute the correlation function according to Eq. (11). As this involves several matrix inversions, it is important to make sure that the matrix determinant is not zero. That means that one cannot use ℓm combinations that are a linear combination of other ℓm's. As all of the pair distributions are real, we cannot keep $m > 0$ and $m < 0$ components at the same time (see Table I). Therefore, we adopt the convention to use only positive components (including $m = 0$ component). Therefore, we remove all functions with negative m from both $\mathbf{T}_q$ and $\mathbf{M}_q$ when solving Eq. (11). One can add the missing negative m components to the correlation function by multiplying the positive m values by the appropriate factor of $(-1)^{\ell+m}$. For consistency, one may repeat the procedure, this time removing the positive m components from $\mathbf{T}_q$ and $\mathbf{M}_q$, and the obtained results should be identical.

We remind the reader that each q bin is independent in $\mathbf{T}_q$, $\mathbf{M}_q$, and $\mathbf{C}_q$. Therefore, solving Eq. (11) can be done for each q bin independently. The starting points then are not vectors of functions, but simply vectors of real numbers $\mathbf{T}_q$ and $\mathbf{M}_q$ and the result is also a vector of real numbers $\mathbf{C}_q$. A covariance matrix $(\boldsymbol{\Delta}^2\mathbf{T})_q$ is in this case a 2D matrix of real numbers, as is the resulting correlation function covariance matrix $(\boldsymbol{\Delta}^2\mathbf{C})_q$. Solution of Eq. (11) then reduces to a problem of solving a set of linear equations, for which many standard numerical algorithms exist. The procedure is repeated for each q bin and the $\mathbf{C}_q$ vector is filled in steps.

III. REALISTIC EXAMPLES

We have tested and applied the formalism to the construction of two-particle correlation functions for identical and nonidentical particles in relativistic heavy-ion collisions. Our tests include a study of the robustness of our approach in the presence of θ-ϕ acceptance holes in relative momentum, a common occurence in experiments including the STAR experiment of which one of the authors (Kisiel) is a collaboration member. Later in this article we present some tests of the method with a realistic model.

A. Example correlation functions

Two particles are femtoscopically correlated if they have a small relative momentum $\mathbf{k}^*$ in the pairs' rest frame (for identical particles we use $\mathbf{q} = \mathbf{k}^*$). If they are not identical and have different masses, they must have different momenta in the laboratory frame. In such case it can happen that because of specific momentum acceptance of the experiment, pairs with specific values of $k^* = |\mathbf{k}^*|$ and certain combinations of polar and azimuthal components of $\mathbf{k}^*$ cannot be measured. In terms of the spherical harmonic representation, this results in a hole in the pair acceptance for certain regions in k^*, ϕ, and $\cos\theta$. This is observed, for example, for pion-kaon pairs in the STAR experiment. Such a hole presents a methodological problem for traditional methods of decomposing the correlation function in spherical harmonics as they rely on the existence of certain symmetries in pair distributions. In particular, they assume that the multiplicity of pairs with a given k^*_{out} is equal to the multiplicity of pairs with $-k^*_{\mathrm{out}}$. For nonidentical particles there is no such symmetry. While it is certainly possible to improve the existing methods and to remove this dependence, we propose to move to the more advanced decomposition method presented in this article and bypass the problem altogether. In our method, this hole is reflected in both the numerator and the denominator by a lower number of pairs contributing at some bins of k^*.

Examples of the numerator of the correlation function, binned directly in spherical harmonics, are shown in Fig. 1. In this case, the distributions result from a simulation of the π^+K^+ correlation function in the THERMINATOR model using the STAR detector acceptance [9]. The acceptance is symmetric with respect to $\cos\theta$, so the $\ell, m = 1, 0$ component vanishes [5]. All the imaginary components vanish. Also the $\ell, m = 2, 1$, as well as $\ell, m = 3, 0$ and $\ell, m = 3, 2$, vanish because of polar angle symmetry. Apart from that, the numerator shows nontrivial structure as a function of both k^* and ϕ. The synergy between spherical harmonic decomposition and femtoscopic correlation function is nicely illustrated in this plot. Full 3D information, which in traditional 3D implementation would require tens of thousands of bins to store, is reduced to a few 1D histograms. Of these, only a select few carry important information, while others conveniently vanish because of the intrinsic symmetries of the pair distribution. The significance of the components diminishes with growing ℓ, ensuring that cutting the decomposition at some ℓ_{max} should not distort the function.

Having in mind that the underlying numerator has a nontrivial structure in both k^* and ϕ, it is interesting to see how the correlation function itself, calculated with the method described earlier in this article, behaves. It is shown in Fig. 2.

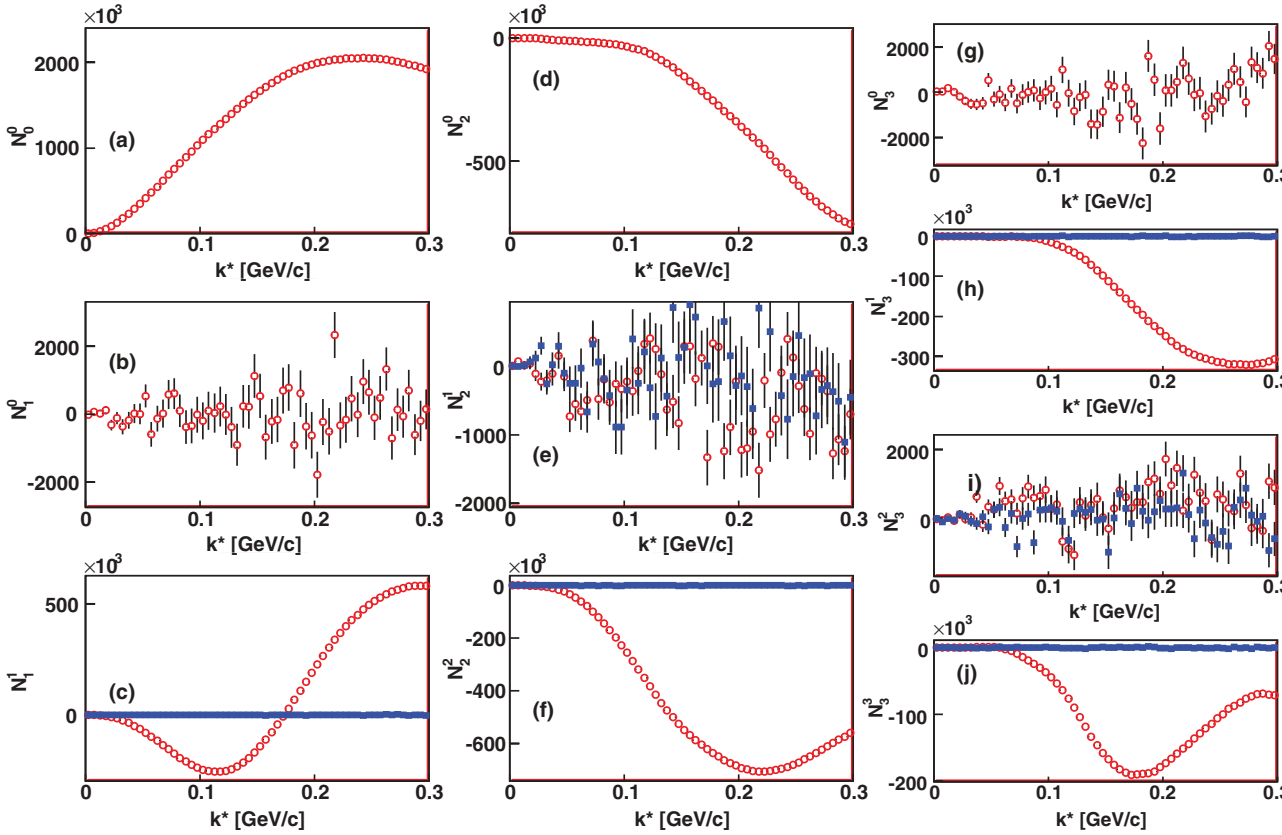

FIG. 1. (Color online) Numerator of an example π^+K^+ correlation function binned directly in spherical harmonics, as a function of the first particle's momentum in the pair rest frame $\mathbf{k}^*$. Panel (a) shows $\ell = 0$; panels (b) and (c) show $\ell = 1$ components; center panels (d)–(f) show $\ell = 2$ components; right panels (g)–(j) show $\ell = 3$ components. Open red circles represent the real part of the decomposition, solid blue squares show the imaginary part.

Again, the imaginary components all vanish, as they should. The C_{00} component shows the expected behavior coming from a Coulomb repulsion of same charge pion and kaon. The C_{20} and C_{22} components show small deviations from zero, which signals the fact that the size of the underlying system is not the same in the out, side, and long directions. Also, the C_{11} component deviates from zero significantly, a signature of the average emission point asymmetry between pions and kaons. In summary, the example confirms several important points: (a) The correlation function can be calculated via the direct $Y_{\ell m}$ method. (b) The important physics signals in C_{00}, C_{11}, C_{20}, and C_{22}, are preserved. (c) Other components of the correlation function vanish, as they should—an important cross-check of the method.

B. Limits of applicability in presence of an acceptance hole

To attempt to determine the practical limits of the technique, we performed a test. First, we calculated the correlation function for identical pions using the THERMINATOR model. We chose to use identical neutral pion pairs for the calculation simply because final-state interactions do not distort the correlation appreciably, meaning that the correlation shape can be characterized simply by the correlation radii $R_{\rm side}$, $R_{\rm out}$, and $R_{\rm long}$. The source size has been set to reasonable values in the longitudinally comoving system (of ∼3–4 fm). The first calculation does not have any acceptance holes. We then repeat the calculation, introducing an artificial hole in the acceptance by removing both from the numerator and denominator all pairs within the hole. The hole is at midrapidity (small $\cos\theta$), small q (from 0.01 to 0.05 GeV/c), and with varying width in ϕ (from 0 to $3\pi/2$). The results are shown in Fig. 3.

One can see that introducing the hole had no influence on the extracted correlation function within statistical errors. Indeed, the dominant effect of the acceptance hole has been to decrease statistics, increasing statistical scatter and the corresponding uncertainty. To further make this point, we show the analytical prediction for what the spherical harmonics should look like for these sizes in the black dashed lines. As one can see, all points follow the lines perfectly.

Our results are in contrast to what would happen in the traditional approach of expanding the correlation in spherical harmonics after making the ratio of 3D histograms. If there is poor statistics because of a gap in acceptance, then one will need a large number of spherical moments to capture the purely statistical fluctations present in the poorly populated high-q bins. What is more insidious, because the correlation is a ratio, the structure in poorly determined 3D bins appear to "cancel out" even when the poorly resolved

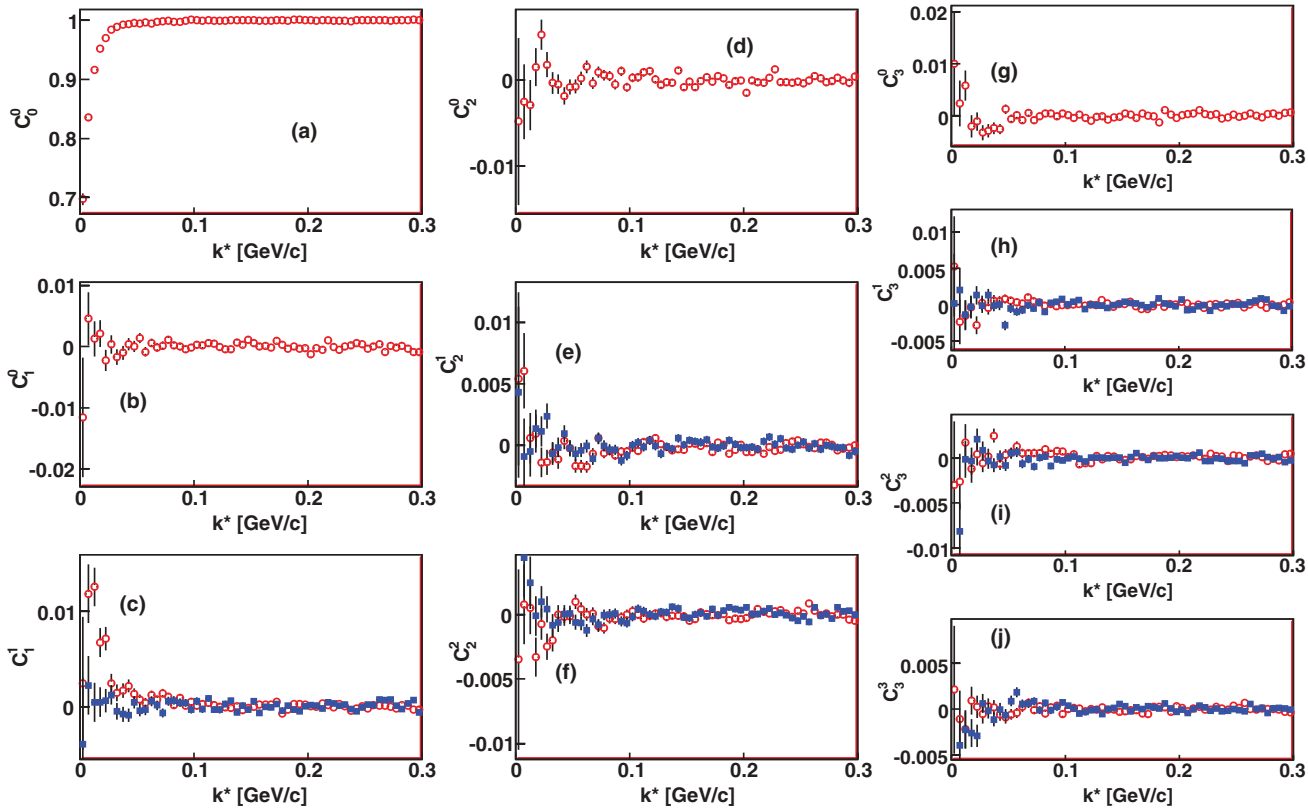

FIG. 2. (Color online) The example correlation function binned directly in spherical harmonics. The open red circles are the real parts of each term and the solid blue squares are the imaginary parts of each term. The spherical moments of the numerator spectra are shown in the panels as they are in Fig. 1.

data should not cancel out. Rather, the poor statistics should give rise to large uncertainties and not contribute to the spherical harmonic expansion (which is what happens in our method).

In Fig. 4, we show the values of the analytical fit to the spherical harmonics vs the hole size. The lines are the "input radii" from the THERMINATOR model. As one sees, the fit results are very stable and moreover in reasonable agreement with the input values. Note that exact agreement between the input and extracted radii cannot be expected because the collective motion in the THERMINATOR model shrinks the effective homogeneity length seen by the pairs and hence the correlation radii. Even with a very large hole of $3\pi/2$ (only a quarter of acceptance remaining) our method seems to preserve all the relevant components, provided that enough statistics remains outside the hole region.

C. Experimental corrections

To to be useful, the procedure for calculating the correlation function directly in spherical harmonics should allow for the application of the standard experimental corrections. Here we describe briefly how this can be done.

Experimental resolution for two-particle reconstruction and identification is usually dominated by two issues: track merging (where two tracks in the detector are reconstructed as one) and track splitting (where a single track is mistakenly reconstructed as two). These have nontrivial dependence on both the particle momenta as well as their trajectory in the detector. This is usually corrected for by assigning a weight to each pair, based on the detailed detector simulation. Such weighting can be incorporated in the procedure in a straightforward way. When filling the numerator and the denominator with pairs, one simply fills it with the appropriate weight. Mathematically, it amounts to modifying Eq. (4) by multiplying the $Y^*_{lm}(\Omega_{\hat{q}_i})$ by an additional weight W, coming from the previously mentioned correction.

Another common issue is the particle purity, namely the fraction of pairs in the sample that should be treated as correlated. A pair may be not correlated if one of the particles is misidentified or if at least one of the particles comes from a weak decay. The experiment should be able to estimate the the average purity of pairs P, which can be (and usually is) a function of particles' momenta, and therefore also of the pair relative momentum $\mathbf{q}$. We use the traditional formula:

$$C_{\mathrm{corr}}(\mathbf{q}) = \frac{C_{\mathrm{meas}}(\mathbf{q}) - 1}{P(\mathbf{q})} + 1. \tag{14}$$

From the correlation function C, we can obtain the correlation effect $R \equiv C - 1$. In spherical harmonic representation, this only modifies the $\ell = 0, m = 0$ component, $R_{00} = C_{00} - 1$, while others remain the same, $R_{\ell m} = C_{\ell m}$. Then Eq. (14)

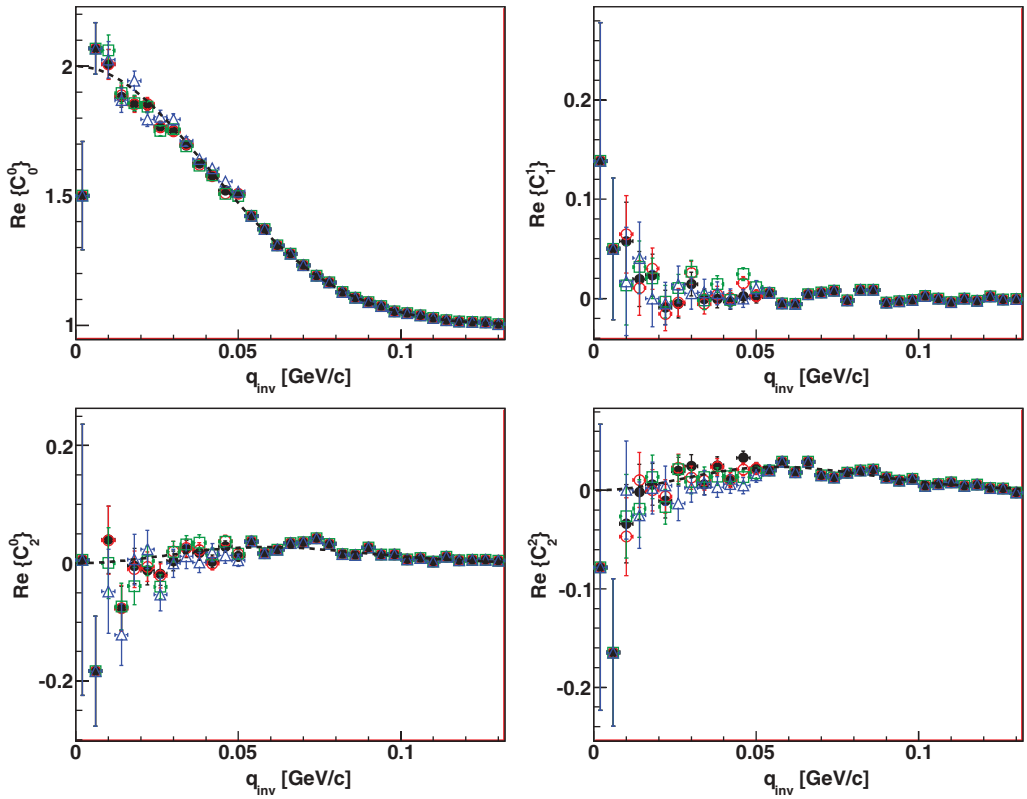

FIG. 3. (Color online) The simulation of the acceptance hole, made at midrapidity (small $\cos\theta$) at small $q = 2k^*$ (from 0.01 to 0.05 GeV/c) and with varying width in ϕ (from 0 to $3\pi/2$). The plot shows the correlation in spherical harmonics for: ideal case with no hole (black diamonds), "small hole" $\pi/6$ (red circles), "sizeable hole" $\pi/2$ (green squares), and "huge hole" $3\pi/2$ (blue triangles). The black dashed lines show the analytical prediction for what the spherical harmonics should look like for these sizes.

simplifies to

$$R_{\mathrm{corr}}(\mathbf{q}) = \frac{R_{\mathrm{meas}}(\mathbf{q})}{P(\mathbf{q})}. \tag{15}$$

We immediately note that it is equivalent to calculating the correlation function from the numerator and denominator. Therefore, it is enough to express purity P directly in spherical harmonics and treat it as the denominator, take the measured correlation function and treat it as the numerator and finally apply the mathematical formalism described in this work to obtain the correlation function corrected for purity.

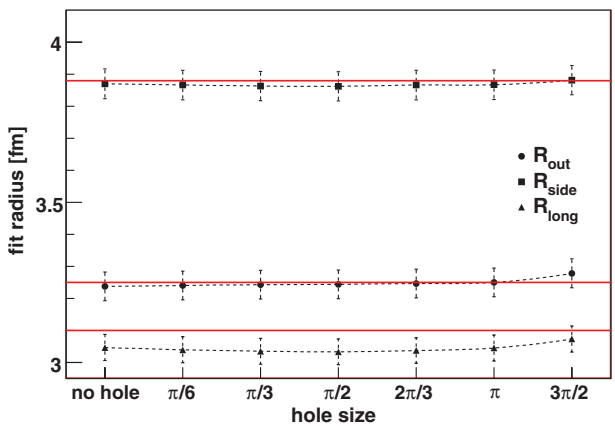

FIG. 4. (Color online) The values of the analytical fit to the spherical harmonics vs the hole size. The solid lines are the "input radii" from the THERMINATOR calculations and the dashed lines/symbols are our fits.

IV. APPLICABILITY

The method presented in this article has been successful applied to the femtoscopic correlation functions in heavy-ion collisions. It should be possible to apply it to other fields as well; however, one has to take into account the limits of the method applicability.

The basic formula (8) is strictly correct, mathematically, only if one uses an infinite number of ℓ, m components for all the functions $\mathbf{T}_q$, $\mathbf{M}_q$, and $\mathbf{C}_q$. In practical application, one needs to limit oneself to a specific value of ℓ. This is allowed only if the higher ℓ moments are negligible. The femtoscopic correlation function is very well suited to the method because the intrinsic symmetries of the pair distributions limit the relevant ℓ components to a practical maximum of six. Most important information is contained in $\ell = 0$, $\ell = 1$, and $\ell = 2$ components.

We have shown that the method remains stable for any reasonable acceptance hole in the ϕ region. It is also clear that the method will start breaking down only for really small values of $\phi - \theta$ acceptance, and in the extreme case of the "hole" taking up the whole $\phi - \theta$ acceptance the method will

simply break down because of a lack of data. The method in effect interpolates the correlation function in the region where there are no data by assuming certain symmetries in the underlying pair distribution. Using the method described here for femtoscopy, acceptance holes are "irrelevant"—any reasonable femtoscopic measurement will have a large-enough acceptance to be insensitive to the holes.

ACKNOWLEDGMENTS

The authors thank Andrew Glenn for his careful reading of the manuscript. This work performed under the auspices of the US Department of Energy by Lawrence Livermore National Laboratory under Contract No. DE-AC52-07NA27344 and US NSF Grant No. PHY-0653432.

[1] B. Tapley, J. Ries, S. Bettadpur, D. Chambers, M. Cheng, F. Condi, B. Gunter, Z. Kang, P. Nagel, R. Pastor, T. Pekker, S. Poole, and F. Wang, J. Geodesy **79**, 467 (2005).

[2] P. Magain, F. Courbin, and S. Sohy, Astron. J. **494**, 472 (1998); F. Courbin, P. Magain, M. Kirkove, and S. Sohy, *ibid.* **529**, 1136 (2000); J. R. Bond, A. H. Jaffe, and L. Knox, Phys. Rev. D **57**, 2117 (1998).

[3] G. Hinshaw *et al.*, Astrophys. J. Suppl. **180**, 225 (2008).

[4] D. Brown, M. Heffner, R. Soltz, and P. Danielewicz, S. Pratt, Phys. Rev. C **72**, 054902 (2005).

[5] Z. Chajecki and M. Lisa, Phys. Rev. C **78**, 064903 (2008).

[6] L. Tenorio, J. A. Scales, and R. Snieder, *Noise, Discretization and Truncation in Inverse Problems*, http://mesoscopic.mines.edu/∼jscales/papers/noise_disc.ps.gz.

[7] J. A. R. Blais and D. A. Provins, J. Geodesy **76**, 29 (2002).

[8] S. Pratt, T. Csörgő, and J. Zimańyi, Phys. Rev. C **42**, 2646 (1990); G. Bertsch, M. Gong, and M. Tohyama, *ibid.* **37**, 1896 (1988).

[9] A. Kisiel, Braz. J. Phys. **37**(3A), 917 (2007).